Effect of anode material and dispersal limitation on the performance and biofilm community in microbial electrolysis cells

Biofilm 6 (2023) 100161

Contents lists available at ScienceDirect

Biofilm

journal homepage: www.sciencedirect.com/journal/biofilm

Effect of anode material and dispersal limitation on the performance and biofilm community in microbial electrolysis cells

Marie Abadikhah [a,*], Ming Liu [b], Frank Persson [a], Britt-Marie Wilén [a], Anne Farewell [c], Jie Sun [d,e], Oskar Modin [a,**]

[a] Water Environment Technology, Architecture and Civil Engineering, Chalmers University of Technology, Gothenburg, Sweden
[b] Key Laboratory of Optoelectronics Technology, Beijing University of Technology, Beijing, 100124, China
[c] Chemistry and Molecular Biology, University of Gothenburg, Sweden
[d] College of Physics and Information Engineering, Fuzhou University, and Fujian Science and Technology Innovation Laboratory for Optoelectronic Information of China, Fuzhou, 350100, China
[e] Microtechnology and Nanoscience, Chalmers University of Technology, Gothenburg, Sweden

ARTICLE INFO

Keywords:
Graphene
Bioanode
Bioelectrochemical system
Metagenomics
Microbial community assembly

ABSTRACT

In a microbial electrolysis cell (MEC), the oxidization of organic compounds is facilitated by an electrogenic biofilm on the anode surface. The biofilm community composition determines the function of the system. Both deterministic and stochastic factors affect the community, but the relative importance of different factors is poorly understood. Anode material is a deterministic factor as materials with different properties may select for different microorganisms. Ecological drift is a stochastic factor, which is amplified by dispersal limitation between communities. Here, we compared the effects of three anode materials (graphene, carbon cloth, and nickel) with the effect of dispersal limitation on the function and biofilm community assembly. Twelve MECs were operated for 56 days in four hydraulically connected loops and shotgun metagenomic sequencing was used to analyse the microbial community composition on the anode surfaces at the end of the experiment. The anode material was the most important factor affecting the performance of the MECs, explaining 54–80 % of the variance observed in peak current density, total electric charge generation, and start-up lag time, while dispersal limitation explained 10–16 % of the variance. Carbon cloth anodes had the highest current generation and shortest lag time. However, dispersal limitation was the most important factor affecting microbial community structure, explaining 61–98 % of the variance in community diversity, evenness, and the relative abundance of the most abundant taxa, while anode material explained 0–20 % of the variance. The biofilms contained nine *Desulfobacterota* metagenome-assembled genomes (MAGs), which made up 64–89 % of the communities and were likely responsible for electricity generation in the MECs. Different MAGs dominated in different MECs. Particularly two different genotypes related to *Geobacter benzoatilyticus* competed for dominance on the anodes and reached relative abundances up to 83 %. The winning genotype was the same in all MECs that were hydraulically connected irrespective of anode material used.

1. Introduction

Microbial electrolysis cells (MECs) have been explored for various applications such as biosensing, recovery of resources from waste streams, and production of chemicals and energy carriers [1,2]. Electrogenic microorganisms, such as those from the *Desulfobacterota* phylum (formerly known as *Deltaproteobacteria*) and more specifically *Geobacter* species, are typically involved in the breakdown of organic material and the following transportation of electrons [3–5]. These microorganisms can be utilized in systems such MECs and other microbial electrochemical technologies (METs) to generate current through the transportation of electrons to the anode surface. The electrons are then transferred to the cathode, where they can be used by the cathode for reduction reactions. These reduction reactions typically lead to the recovery of different resources, e.g., hydrogen or methane gas [6–9].

* Corresponding author.
** Corresponding author.
E-mail addresses: marie.abadikhah@chalmers.se (M. Abadikhah), oskar.modin@chalmers.se (O. Modin).

https://doi.org/10.1016/j.biofilm.2023.100161
Received 9 August 2023; Received in revised form 5 October 2023; Accepted 8 October 2023
Available online 10 October 2023

Various factors affect the microbial community composition and the function of METs. Deterministic factors such as substrate composition, electrode materials, and system design will select for specific species, which are fit to survive in the system [5,10,11]. Stochastic factors such as ecological drift and diversification will cause differences in microbial community composition and function between systems that operate under the same environmental conditions. For example, Zhou et al. [12] showed that stochastic initial colonization caused differences in both community structure and function in MECs operated under identical conditions. Dispersal limitation increases stochasticity and leads to differences in microbial communities exposed to identical selection pressures whereas high dispersal rates reduces community differences [13]. The relative importance of deterministic and stochastic factors in shaping the microbial communities and how this relates with the function of the METs under various conditions is still not known.

The anode material is one factor that affects the microbial community and electrical current generation in METs. Conventionally, METs use carbon-based materials since metals tend to corrode in aquatic environments [14,15]. Some commonly used materials are carbon paper, carbon felt and carbon cloth [16,17]. Graphene is a highly conductive two-dimensional carbon-based material, which has been shown to have a large surface area and that could be produced at low cost [18–20]. Some previous studies have used graphene-based electrodes in METs with promising results. For example, they were shown to increase the power density in microbial fuel cells and the hydrogen production in MECs in comparison to conventional materials [21–23]. In other systems, graphene covered surface has been shown to have an antimicrobial effect. In forward osmosis membranes for water treatment, graphene coating has reduced biofouling [24–26]. The physiochemical and antimicrobial properties of some forms of graphene have also been highlighted within biomedical applications, such as in preparation of substrates for tissue engineering as well as drug delivery [27,28]. In METs, it is unknown how graphene-based anodes affect the microbial community composition in comparison to other materials and if the deterministic effect of the anode material is large or small in comparison to stochastic factors.

The aim of this study was to determine if differences in anode materials affect current generation and microbial community composition in single-chamber MECs, and if this effect is larger or smaller than stochastic factors. We compared three anode materials: carbon cloth, graphene, and nickel. We examined stochastic factors by enabling homogenizing dispersal between some MECs and completely blocking dispersal between others. We found that the anode material was the dominating factor affecting the lag phase and current generation in the MECs, but stochastic factors were more important for microbial community assembly of biofilms on the anode surfaces.

2. Material and methods

2.1. Production of graphene electrodes

The vertical graphene was grown onto physical vapour deposited (PVD) nickel thin films on silicon samples with 300 nm thick thermal SiO_2 layers. The graphene growth was performed in a plasma enhanced chemical vapour deposition (PECVD) system. The deposition atmosphere in the chamber was C_2H_2:H_2:Ar = 25:16:285, and the temperature was 830 °C. The pressure in the growth chamber was 8 mbar and the growth lasted 5 min in a local plasma at 100 kHz and 50 W. The as-grown vertical graphene thin film is sponge like, with numerous interconnected graphene flakes (not necessarily monolayers) pointing approximately upwards (perpendicular to the substrates). The vertical graphene thin film is about 1 μm thick (film thickness, not the individual flake thickness). Samples with bare Ni/SiO_2/Si substrates are used as the control samples.

2.2. Microbial electrolysis cells (MECs)

Twelve single-chamber MECs with the internal dimensions of 3 × 1.5 × 1 cm^3 were constructed. Each MEC had two circular, 1-cm diameter electrodes, each with a surface area of 0.79 cm^2. The two electrodes were facing each other and placed 1 cm apart. One electrode served as anode, and one served as cathode in each MEC. All cathodes were stainless steel plates (EN 1.4301). Four of the MECs had anodes made of carbon cloth (AvCarb 1071 HCB, Fuelcellearth.com), four had anodes of vertical graphene flakes coated on a nickel support layer using chemical vapour deposition as explained above, and four had anodes with only the nickel support layer without the graphene flakes (i.e., the control samples mentioned above).

The MECs were placed in four liquid loops, each loop containing three MECs with different anode materials (Fig. 1). Each loop was connected to a 200 mL glass flask with an attached gas bag. The glass flask contained a nutrient medium (NM) that was recirculated through the three MECs and back to the flask using a peristaltic pump operating at a flow rate of 40 mL/min. One such system with a glass flask and three MECs is referred to as a hydraulic loop. The total liquid volume in each loop was 225 mL. The recirculation of liquid enabled dispersal of microorganisms between MECs within the same hydraulic loop, but no dispersal could occur between MECs placed in different hydraulic loops.

The graphene, nickel, and carbon cloth anodes are referred to with the letters G, N, and C, respectively. The hydraulic loops are referred to with the numbers 1–4. Thus, the graphene anode in hydraulic loop 1 is labelled G1, etc.

The nutrient medium (NM) consisted of 0.1 g/L KCL, 0.6 g/L KH_2PO_4, 0.25 g/L NH_4CL, 3 g/L $NAHCO_3$, 0.1 g/L $MgCl_2$ and 0.03 g/L $CaCl_2$ [29] and trace mineral solution [30].

2.3. Operation

Each hydraulic loop was inoculated with 24 mL mesophilic anaerobic digester sludge. This was mixed with NM made in accordance to Ref. [29], with the addition of trace mineral solution [30]. The NM media was supplemented with sodium acetate (0.60 g/L), sodium propionate (0.40 g/L), and sodium butyrate (0.32 g/L). These volatile fatty acids were chosen because they are major products from the fermentation of organic material. During operation, 150 mL of the NM was replaced every four days. During replacement, clamps were attached to the tubes to prevent air from entering the hydraulic loops and after addition of fresh NM, the flask were sparged with nitrogen gas for 1–2 min to eliminate any air before restarting the circulation. A cell potential of 1 V was kept between the anode and cathode in each MEC using a multichannel potentiostat (PalmSens). The hydraulic loops were operated for 57 days.

2.4. Analytical methods

A high-performance liquid chromatograph (HPLC) equipped with a UV detector (Shimadzu) and an Aminex HPX-87H ion exclusion column (BioRad) was used to measure the concentrations of acetate, propionate, and butyrate. Cyclic voltammetry (CV) was used to examine the bioelectrochemical activities of the electrodes in each MEC. An Ag/AgCl electrode (BAS inc) was used as reference. All CV measurements were performed 30 min after addition of fresh NM, and the circulation was also stopped during this time. For all measurements, three consecutive scans were performed at a scan rate of 5 mV/s.

2.5. Microbial community analysis

Biofilm growing on all twelve anodes were harvested at the end of the experiment and stored at −20 °C until DNA extraction was done. The biofilm was obtained by scraping the entire anode surface with a sterile laboratory spatula. The DNA extraction was performed using the

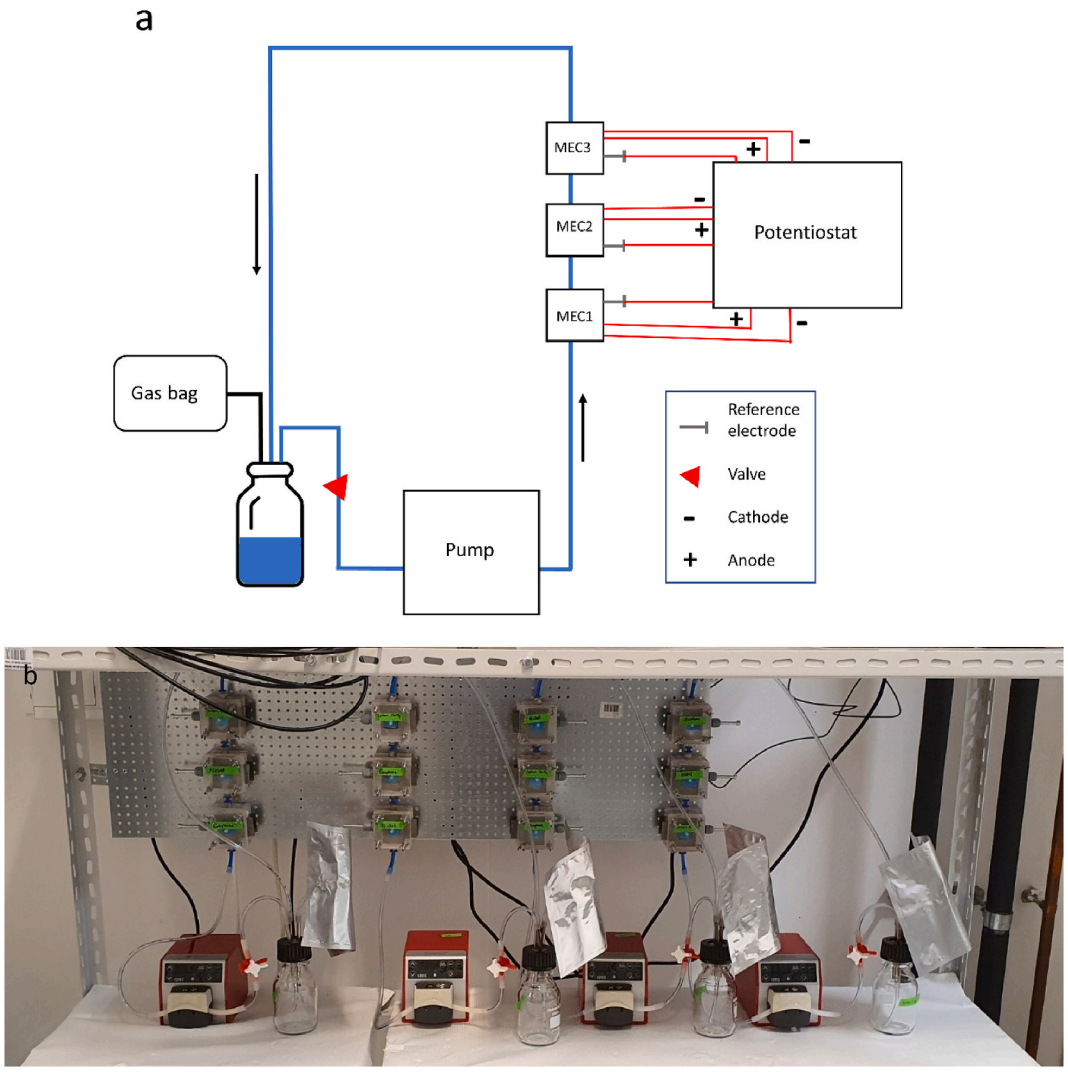

Fig. 1. a) Schematic illustration of one hydraulic loop. **b)** Photograph of the experimental setup.

FastDNA Spin kit for Soil (MP Biomedicals) following the manufacturer's protocol except the homogenization step which was repeated. SMARTer ThruPLEX DNA-seq Kit (cat# R400676, Takara) with HT dual indexes (cat# R400660, Takara) was used to prepare sequencing libraries from 10 to 50 ng of DNA in accordance with the manufacturers' instructions (guide#112219). A Covaris E220 system was used for fragmentation targeting an insert size of 350–400 bp. Paired-end 150 bp read length sequencing was done using NovaSeq 6000 system (Illumina, Inc), S4 flowcell and v1.5 sequencing chemistry.

Quality filtering on the obtained sequencing data was done with fastp v0.20.0 [31], followed by normalization to a target depth of 100 using BBNorm (BBMap v38.61b, https://sourceforge.net/projects/bbmap/). To obtain higher quality bins, the sequence data was processed in two ways: (i) co-assembly using Megahit v1.2.9 [32], read mapping using Bowtie v2.3.5.1 [33], followed by binning using Metabat v2.12.1 [34] and (ii) individual assembly of each sample using Megahit, read mapping using Minimap v2.24-r1122 [35], followed by binning using Vamb v3.0.2 [36]. The obtained bins from both the co-assembly and individual assembly were combined, checked for completeness and contamination using CheckM v1.1.3 [37], and dereplicated using dRep v3.4.0 with an average nucleotide identity (ANI) threshold of 0.95 to obtain species representative genomes. CoverM v0.6.1 (https://wwood.github.io/CoverM/coverm-genome.html) was used to calculate the relative abundance of each species representative in each sample. A bin was considered present in a sample if at least 50 % of its bases were covered by one or more reads.

Taxonomic information was assigned using the GTDB toolkit [38]. Furthermore, bins classified in the Desulfobacterota phylum were compared to genomes belonging to the families Geobacteraceae, Desulfuromonadaceae, Syntrophotaleaceae, and Desulfovibrionaceae downloaded from NCBI using ncbi-genome-download (https://pypi.org/project/ncbi-genome-download). Average nucleotide identities (ANI) and average amino acid identities (AAI) between the bins and the genomes were determined using fastANI v1.33 [39] and fastAAI v0.1.18 (https://github.com/cruizperez/FastAAI), respectively.

Raw sequence reads were deposited at NCBI short read archive (BioProject PRJNA839919).

2.6. Statistical analysis

The effects of anode material and dispersal limitation (i.e., hydraulic loop) on parameters related to both bioelectrochemical anode performance and microbial community structure were investigated. The parameters related to anode performance were lag time, current density, and electrical charge produced in the system. Lag time was defined as the time from inoculation to the generation of a current density of at least 1 A/m^2. Current density was calculated by dividing the generated current with the anode surface area. Electrical charge was calculated using Eq. (1).

$$Charge = \int_0^t I \bullet dt \quad \text{(Eq. 1)}$$

Charge is in coulombs, I is the current in ampere, and t is the time duration in seconds of the time period of interest.

The parameters related to microbial community structure were diversity, evenness, and the relative abundance of the MAGs in the biofilms. Diversity was calculated using the Hill-based framework [40,41], evenness was measured as Pielou's index [42], and the relative abundances of MAGs were obtained using CoverM as described above.

The effects of anode material and hydraulic loop (explanatory variables) on the performance- and microbial community structure parameters (response variables) were assessed using ANOVA and dominance analysis. To examine whether the effects of anode material and hydraulic loop on response variables were statistically significant, two-factor ANOVA was carried out using Statsmodels v0.13.2 [43]. This was followed by paired-sample t-tests as post-hoc analysis using Scipy v1.9.1 [44]. Furthermore, multiple linear regression and dominance analysis [45] was used to assess the percentage contribution of the explanatory variables on the response variables. This was done with the Python packages dominance-analysis (https://github.com/dominance-analysis/dominance-analysis) and pandas [46]. Since both anode material and hydraulic loop are categorical explanatory variables, they were encoded as dummy variables using the pandas.get_dummies function. Then, dominance analysis was used to calculate the percentage contribution of each explanatory variable to the variance of the response variables. The coefficient of determination (R^2) subtracted from one was the unexplained variance while the percentage contribution of each explanatory variable multiplied by the R^2 value was the variance explained by that variable.

Overall community composition was explored using a principal coordinate analysis (PCoA) on dissimilarity matrices calculated using the Hill-number framework and permanova was used to determine statistically significant effects of system and anode material on overall community composition. The python package qdiv v2.2.1 was used for calculation of microbial diversity, evenness, dissimilarity [41] and the adonis2 function in the R package vegan was used for permanova [47,48].

3. Results

3.1. Anode material affected lag time, current density, and charge generation

The current generation during the experiment can be seen in Fig. 2a. A gradual increase in produced current could be observed for all MECs until they reached their peak current generation. Most of the carbon cloth MECs reached a peak current density on day 20. Graphene and nickel both reached a peak current between day 25 and 45, after which a gradual decrease in current density could be observed in some MECs (Fig. 2a).

The lag time before current production began differed between the different materials, ranging from 8 to 38 days (Fig. 2b). Carbon cloth MECs all had the shortest lag times and the smallest variation between MECs in different hydraulic loops. They also generated the highest cumulative electrical charge during the experiment (Fig. 2c). Graphene- and nickel MECs showed much more variation in current density and had longer lag times.

There was a statistically significant effect of anode material on lag time, peak current density, and total charge generated during the experiment ($p < 0.05$, ANOVA), but no significant effect of the hydraulic loop. A difference between carbon cloth and the other materials was found from the post-hoc test ($p < 0.05$, *t*-test). When the data was assessed for each week of the experiment, a significant effect of the hydraulic loop on peak current density could be observed during the 3rd week (day 7–20) ($p < 0.05$). Post-hoc analysis identified a difference between hydraulic loop 1 and 4 ($p < 0.05$, *t*-test). In Fig. 2a, a rapid start-up of current generation is observed for all anode materials in hydraulic loop 1, while the graphene and nickel anodes had long lag times in hydraulic loop 4.

Availability of organic substrate was not limiting in the hydraulic loops as NM was replenished every 4 days and the concentrations of acetate, propionate, and butyrate fluctuated between 0.4 and 10.5 mM (Fig. S1, Supplementary material). Near day 30 and 50, some of the recorded data were lost because of malfunctioning equipment, which explains the gaps in Fig. 2.

Comparison of CV tests at the start and end of the experiment shows clear differences for all materials, indicating bioelectrochemical activity on the anode surface (Fig. 3), which is consistent with the observations of current density in the MECs (Fig. 2a). The CVs also showed that

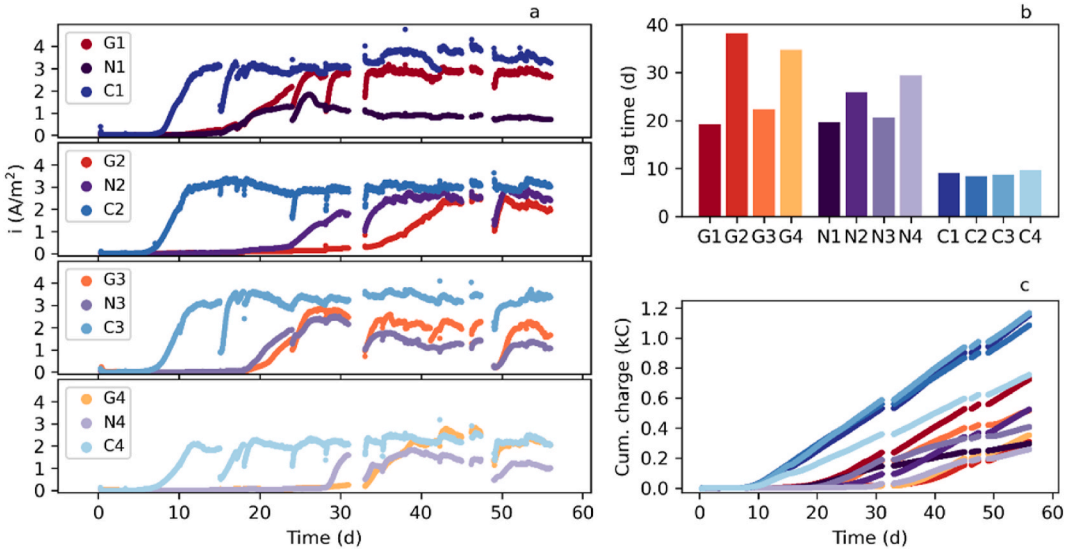

Fig. 2. a) Current density during the experimental run. G1-G4 are the MECs with graphene anodes, N1–N4 are the MECs with nickel anodes, and C1–C4 are the MECs with carbon cloth anodes. The numbering for each MEC refer to the system in which it is located. **b)** A bar graph depicting the number of days before each reactor started producing current (at least 1 A/m^2). **c)** The cumulative charge generated in each MEC.

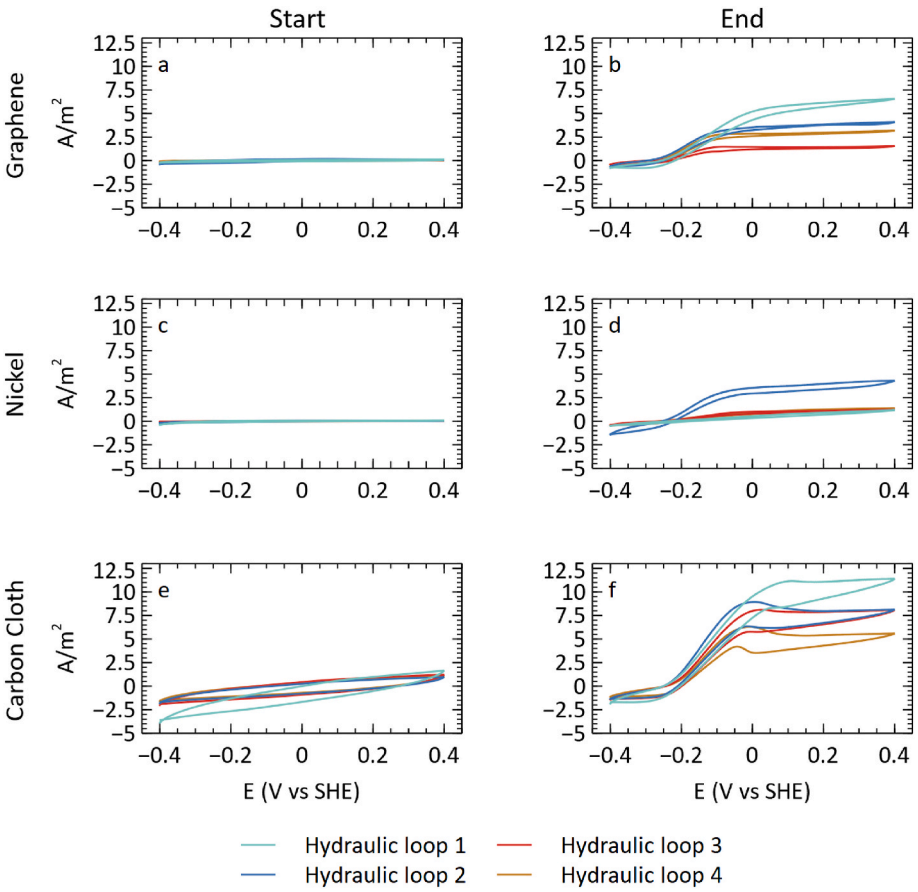

Fig. 3. Cyclic voltammetry measurements of the anodes from the start (a, c, e) and end (b, d, f) of the experiment. Graphene (a, b), nickel (c, d), and carbon cloth (e, f) are shown in different panels while hydraulic loops are indicated by colour of the lines. (For interpretation of the references to color in this figure legend, the reader is referred to the Web version of this article.)

carbon cloth anodes had a greater ability to catalyse bioelectrochemical reactions in comparison to the other materials.

3.2. *Desulfobacterota* species dominated the anode biofilms

In total, metagenomic analysis resulted 1184 bins, which were dereplicated into 164 species-representative genomes in the anode biofilms. Out of these, 79 were high quality MAGs with completion >90 % and contamination <5 %, 75 were medium quality MAGs with >50 % completion and <10 % contamination, and 10 were low quality bins with contamination exceeding 10 %. The 26 most abundant MAGs, having a relative abundance >1 % in a sample or a mean relative abundance >0.2 % are shown in Fig. 4. These MAGs accounted for 74–92 % of the reads from the anode biofilm communities.

Desulfobacterota was the most abundant phylum with 10 MAGs in the dataset, making up 64–90 % of the communities. Particularly two *Geobacter* spp. were found in high relative abundance on the anodes. One species (S71_927) dominated in all MECs in hydraulic loop 1. Another species (S78_1107) dominated in the other three hydraulic loops. The two species had an ANI of 90 % and an AAI of 83 %. When compared to reference genomes from NCBI, both were most similar to *Geobacter benzoatilyticus*, NZ_CP071382.1 [49], with S71_927 having 91 % ANI and 87 % AAI to this genome, and S78_1107 having 94 % ANI and >90 % AAI. The unclassified *Geobacter* MAG S74_483 was most similar to *Geobacter hydrogenophilus* (NZ_JAHCZI010000010.1) with 86 % ANI. The three *Trichloromonas* MAGs were most similar to *Desulfuromonas acetexigens* (NZ_FOJJ01000041.1) with 89–90 % ANI. The two MAGs in the *Pseudopelobacteraceae* family were not closely related to any of the reference genomes with 78 % ANI to *Pelobacter propionicus* (NC_008609.1). All biofilms also contained MAGs within the phyla *Actinobacteriota, Bacteroidota, Firmicutes, Proteobacteria*, and *Spirochaetota* (Fig. 4).

A statistically significant effect of the hydraulic loop was observed on the relative abundance of 30 MAGs and of anode material on 4 MAGs ($p < 0.05$, ANOVA). Among the most abundant MAGs, 5 were affected by the hydraulic loop and 1 by material (Fig. 4).

3.3. The hydraulic loop affected biofilm community structure, anode material did not

Fig. 5a–d shows the alpha diversity as Hill numbers with diversity order 0, 1, and 2 [50] and the evenness. The ^{0}D is equivalent to richness, the number of taxa detected in each sample, which ranged from 40 to 107. The values for ^{1}D and ^{2}D were 1.9–7.4 and 1.3–3.2, respectively, and the evenness ranged from 0.17 to 0.44There was a statistically significant effect of hydraulic loop on the ^{2}D and evenness indices ($p < 0.05$, ANOVA). Particularly hydraulic loop 1, which was dominated by the *Geobacter* S71_927 MAG, had lower diversity and evenness than the other hydraulic loops ($p < 0.05$, *t*-test).

Fig. 5e–g shows PCoA ordination of dissimilarity matrices calculated using the Hill-based framework with diversity orders 0, 1, and 2 [41]. Statistical analysis using permanova showed that the hydraulic loop had a significant effect on the community composition of all three dissimilarity indices ($p < 0.05$), but anode material did not.

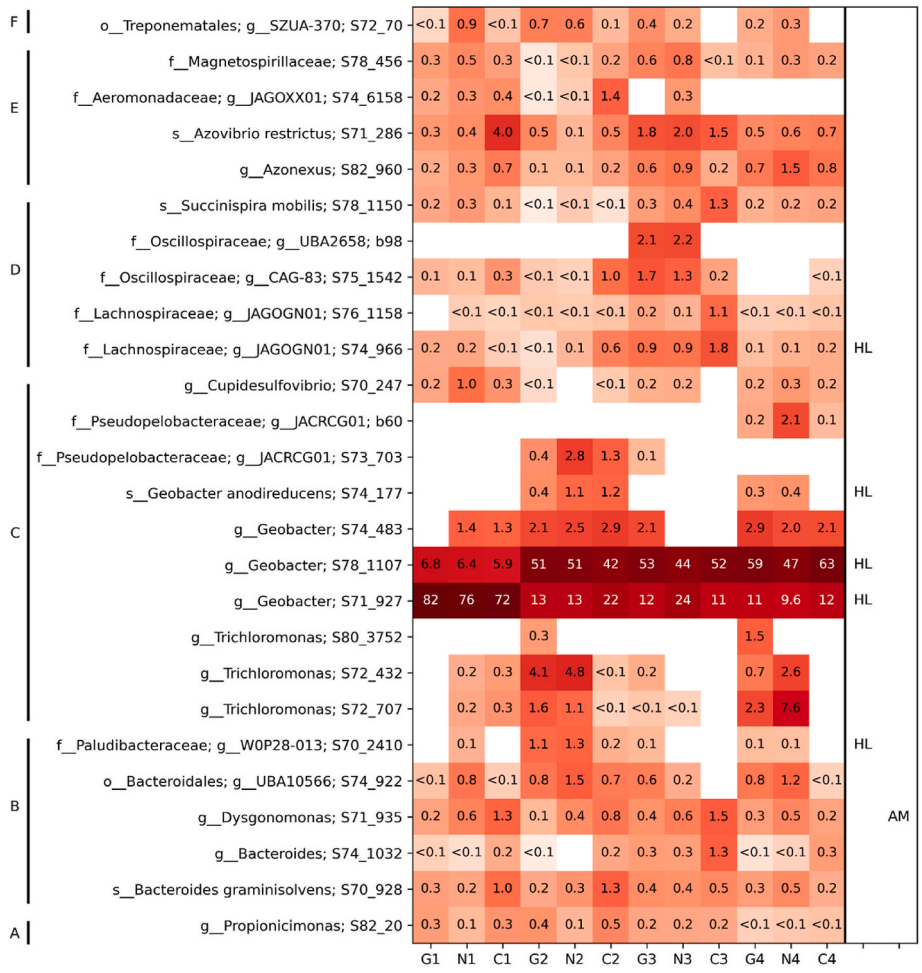

Fig. 4. Relative abundance (%) of the most abundant MAGs in the anode biofilms. The MAGs are grouped based on phylum: *Actinobacteriota* (A), *Bacteroidota* (B), *Desulfobacterota* (C), *Firmicutes* (D), *Proteobacteria* (E), and *Spirochaetota* (F). Taxonomy is based on GTDB Release 07-RS207. Statistically significant effect on the relative abundances of the MAGs by either hydraulic loop (HL) or anode material (AM) is shown in the right panel ($p < 0.05$, ANOVA).

3.4. Anode material explained most of the variance in bioelectrochemical performance while hydraulic loop explained the variance in microbial community structure

Dominance analysis shows the relative contributions of explanatory variables to the variance of a response variable in multiple regression [45]. Fig. 6 shows that anode material explained most of the observed variance in lag time, peak current density, and total electrical charge generated in the MECs. On the other hand, hydraulic loop explained most of the variance in diversity (^{1}D, ^{2}D) and evenness, as well as the relative abundance of several of the highly abundant taxa in the biofilms, including three of the most abundant *Geobacter* spp.

4. Discussion

4.1. Current generation

There were differences observed in the initial current generation between the different materials. Carbon cloth had a much shorter start-up time in comparison to both graphene and nickel. All four replicates for carbon cloth also had similar start-up times while the other materials showed a large variation. Carbon cloth was the most hydrophobic material (Fig. S2, Supplementary material), which may have facilitated the initial attachment of microbial cells [51]. The slow start-up time and variation of graphene could be attributed to the structure of the graphene. The graphene used in this setup consists of sharp vertical flakes. When the initial colonization of the surface occurs, the bacteria may be pierced by the graphene flakes leading to cell death [52]. The build-up of organic material by the previous bacteria that tried to colonize the surface allows for subsequent bacteria to attach without being pierced by the sharp graphene flakes [52,53]. The variation can also be explained by the stochastic process involved in the initial colonization of the surface [54]. Some studies have shown the importance of stochastic processes in the community assembly within MECs [12] and in other systems such as anammox biofilms [55].

Current density and charge generation varied between the different anode materials. The carbon cloth MECs had the highest current density in all hydraulic loops. The graphene MECs were second best, except in hydraulic loop 2 (Fig. 2). Typically, the current generation in the MEC decreased somewhat after it had reached its peak and was then relatively stable for the remainder of the experimental run. In the early stages of microbial assembly on the anode surface there is a thin layer of biofilm. This allows bacteria to have direct physical contact with the anode surface as well as easy access to the organic substrates in the liquid, resulting in high current generation. Once the biofilm becomes thicker, as both electrogenic and non-electrogenic bacteria attach onto the biofilm, the access to organic compounds become diffusion-limited [56]. Competition for the organic substrates and nutrients between the electrogenic and non-electrogenic bacteria also limits the access to the substrates. There are, however, methods that some of the electrogenic bacteria could potentially employ to overcome the limited access to organic substrates. *Geobacter sulfurreducens*, a bacterium commonly

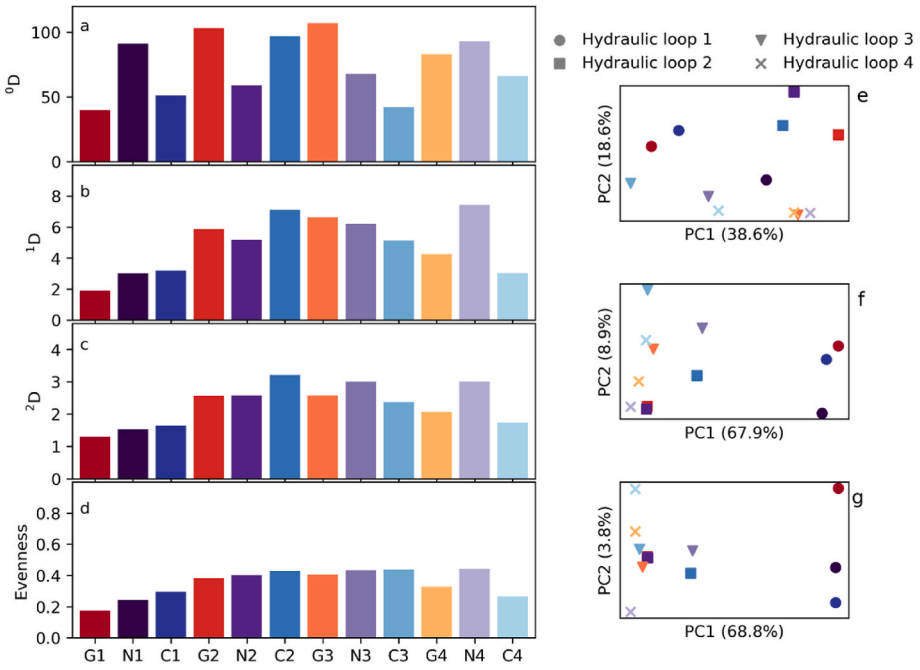

Fig. 5. a-c) Diversity calculated as Hill numbers with diversity order 0 (a), 1 (b), and 2 (c); d) evenness; and e-f) PCoA ordination based on dissimilarity matrices calculated with diversity order 0 (e), 1 (f), and 2 (g). The colors in a-d corresponds to the colors in e-g. (For interpretation of the references to color in this figure legend, the reader is referred to the Web version of this article.)

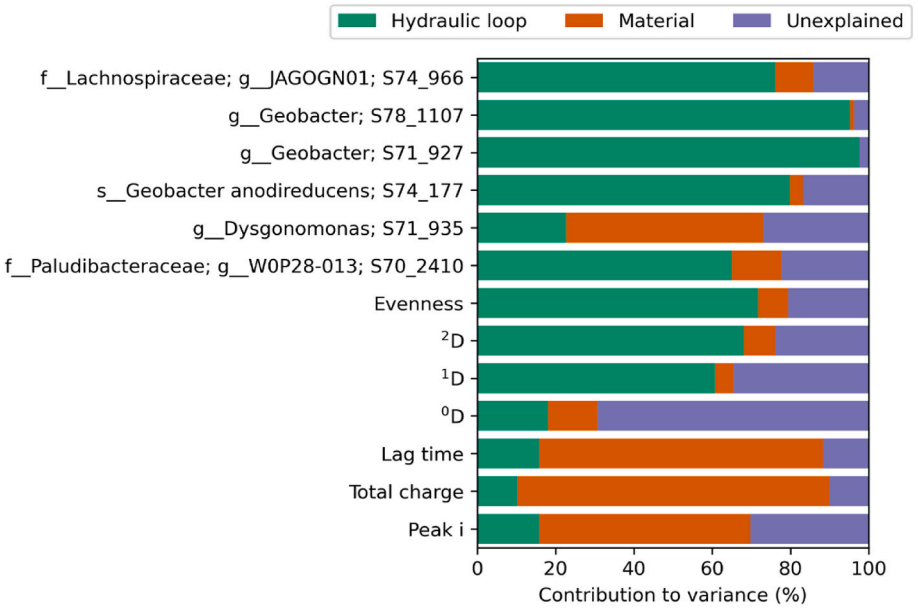

Fig. 6. Dominance analysis showing the contribution of the explanatory variables hydraulic loop and anode material to the variance of several response variables.

found in METs, has been shown to use structures such as nanowires, c-type cytochromes, as well as mediators to aide its transfer of electrons to the anode [57,58]. This would allow electrogens not directly connected to the anode surface to utilize its ability to transfer electrons and contribute to the overall current generation. There is a number of studies that have highlighted the improved performance of METs with graphene electrodes [21,59], as well as some studies that have highlighted the antimicrobial abilities of graphene in other applications [26,27,60]. It seems that the biocompatibility of graphene is dependent on the structure of the graphene sheets used as well as the graphene manufacturing process [15,61,62]. A reason for the reduced performance of the graphene MECs in this study may be due to a layer of dead cells closest to the electrode surface. This layer could result in the lower ability of the graphene to produce equally high levels of current as the carbon cloth. A potential explanation for this could be that not only are the dead cells preventing the direct contact of the viable electrogens with the electrode surface, but they are also limiting the use of other methods to facilitate electron transfer to the electrode surface. The greater performance of the carbon cloth MECs could be attributed to the structure of the carbon cloth, which has been shown to have a good biocompatibility [63,64]. Nickel is known to have a good electrical conductivity and has been shown to improve performance in MFC when used to reinforce graphite electrodes [65]. However, it was observed in this study that the nickel MECs, by itself did not perform as well as the carbon cloth MECs.

4.2. Microbial community diversity and composition on the anodes

The diversity indices showed that although 40–107 MAGs could be detected on the bioanode, most had low relative abundance. The ^{1}D and ^{2}D indices can be interpreted as the number of common and abundant taxa, respectively [66]. The low values, 1.9–7.4 for ^{1}D and 1.3–3.2 for ^{2}D, as well as the low evenness (Fig. 4) show that the biofilm communities are dominated by a few MAGs with high relative abundance.

The microbial community was dominated by *Desulfobacterota,* which are known as electrogens often present in bioelectrochemical systems [67]. The two most abundant MAGs were most closely related to *Geobacter benzoatilyticus*, which was recently isolated from petroleum-contaminated soil. *G. benzoatilyticus* was shown to reduce ferrihydrite, which suggests it can use solid electron acceptors. It was also shown to oxidize acetate, but not propionate [49]. The two dominating MAGs may, thus, use acetate as electron donor for generating electrical current on the anode surfaces. *Trichloromonas* species, which were identified to be similar to *Desulfuromonas acetexigens*, were also present. *Trichloromonas* have been shown to be capable of electron transfer, indicating they are electrogenic bacteria [68]. For instance, *Desulfuromonas acetexigens* have been shown to be involved in the current generation on graphite electrodes through its ability to use acetate as an electron donor [69]. Propionate and butyrate in the NM are likely used by fermentative bacteria. Several fermentative bacteria were found in the biofilms; for instance, *Succinispira mobilis* [70] and MAGs within *Oscillospiraceae* and *Lachnospiraceae*.

4.3. Ecological mechanisms

All anodes were dominated by *Desulfobacterota* species, which is consistent with previous studies showing that bioelectrochemical systems having an acetate-containing feed with near-neutral pH and low to moderate salinity and temperature are highly selective for members of this phylum, particularly *Geobacter* [9]. However, the community structure and the species that dominate in each anode biofilm appears to be governed by stochastic factors such as initial colonization and drift. In the PCoA, the samples separated more based on hydraulic loop than based on anode material, especially when more emphasis is placed on taxa with high relative abundance (Fig. 5f–g). Typically, it might be expected that different microorganisms would randomly attach and colonize the different anode materials within the same hydraulic loop. Instead, it was observed that the anode communities within the same loop had a more similar microbial community structure than those with the same anode material in different loops. This indicates a potential influence of the MEC that was first colonized in each hydraulic loop. The carbon cloth anodes had the shortest lag times and generally the highest DNA concentrations (Fig. 2; Table S1), suggesting that they were colonized early in each loop and developed the thickest biofilms. Based on this, it is likely that dispersal of microorganism from the carbon cloth anode resulted in the colonization of the other MECs in the same hydraulic loop.

The dominance analysis showed that variation in the most abundant electrogene as well as diversity and evenness metrics were mainly due to hydraulic loop and not material, underscoring that stochasticity was involved in the microbial assembly and development of the microbial communities. Anode biofilms that were present in the same system, i.e., the same hydraulic loop, were subjected to homogenizing dispersal and had higher similarity in community composition than anode biofilms in separate hydraulic loops.

5. Conclusions

Four replicate hydraulic loops consisting of three MECs, each with a different anode material, were operated for 56 days. The anode materials consisted of carbon cloth, graphene, and nickel. MECs with carbon cloth had the lowest lag time as well as the highest current generation and total charge generated of the three anode materials. The microbial community analysis showed that *Geobacter* spp. dominated all anode biofilms; however, the species that dominated and the diversity and evenness of the communities differed between MECs. MECs placed within the same hydraulic loop had more similar community composition that MECs in different loops, which showed that stochastic factors such as initial colonization and drift affected community structure.

CRediT authorship contribution statement

Marie Abadikhah: Conceptualization, Methodology, Investigation, Visualization, Formal analysis, Writing – original draft. **Ming Liu:** Investigation, Writing – review & editing. **Frank Persson:** Writing – review & editing. **Britt-Marie Wilén:** Writing – review & editing. **Anne Farewell:** Writing – review & editing. **Jie Sun:** Resources, Writing – original draft. **Oskar Modin:** Conceptualization, Methodology, Funding acquisition, Writing – original draft.

Declaration of competing interest

The authors declare that they have no known competing financial interests or personal relationships that could have appeared to influence the work reported in this paper.

Data availability

The datasets presented in this study can be found in online repositories. The name of the repository and accession number can be found in the article.

Acknowledgements

Sequencing was performed by the SNP&SEQ Technology Platform in Uppsala. The facility is part of the National Genomics Infrastructure (NGI) Sweden and Science for Life Laboratory. The SNP&SEQ Platform is also supported by the Swedish Research Council and the Knut and Alice Wallenberg Foundation. Part of the bioinformatic work was enabled by resources provided by the Swedish National Infrastructure for Computing (SNIC) at UPPMAX partially funded by the Swedish Research Council through grant agreement no. 2018–05973. The project was supported by funding from FORMAS (project 2018-00622) and the J. Gust. Richert foundation (2022-00757). J. Sun acknowledges the support from Fujian provincial projects (Nos. 2021HZ0114, 2021J01583, 2021L3004), and Mindu projects (Nos. 2021ZZ122, 2020ZZ110).

Appendix A. Supplementary data

Supplementary data to this article can be found online at https://doi.org/10.1016/j.bioflm.2023.100161.

References

[1] Escapa A, San-Martín MI, Morán A. Potential use of microbial electrolysis cells in domestic wastewater treatment plants for energy recovery. Front Energy Res 2014;2.
[2] Modin O, Aulenta F. Three promising applications of microbial electrochemistry for the water sector. Environ Sci J Integr Environ Res: Water Research & Technology 2017;3(3):391–402.
[3] Yates MD, Kiely PD, Call DF, Rismani-Yazdi H, Bibby K, Peccia J, Regan JM, Logan BE. Convergent development of anodic bacterial communities in microbial fuel cells. ISME J 2012;6(11):2002–13.
[4] Kokko M, Epple S, Gescher J, Kerzenmacher S. Effects of wastewater constituents and operational conditions on the composition and dynamics of anodic microbial communities in bioelectrochemical systems. Bioresour Technol 2018;258:376–89.
[5] Koch C, Huber KJ, Bunk B, Overmann J, Harnisch F. Trophic networks improve the performance of microbial anodes treating wastewater. npj Biofilms and Microbiomes 2019;5(1):27.

[6] Shin HJ, Jung KA, Nam CW, Park JM. A genetic approach for microbial electrosynthesis system as biocommodities production platform. Bioresour Technol 2017;245(Pt B):1421–9.
[7] De Vrieze J, Arends JBA, Verbeeck K, Gildemyn S, Rabaey K. Interfacing anaerobic digestion with (bio)electrochemical systems: potentials and challenges. Water Res 2018;146:244–55.
[8] Mateo S, Cañizares P, Fernandez-Morales FJ, Rodrigo MA. A critical view of microbial fuel cells: what is the next stage? ChemSusChem 2018;11(24):4183–92.
[9] Logan BE, Rossi R, Ragab Aa, Saikaly PE. Electroactive microorganisms in bioelectrochemical systems. Nat Rev Microbiol 2019;17(5):307–19.
[10] Wang J, Song X, Wang Y, Abayneh B, Ding Y, Yan D, Bai J. Microbial community structure of different electrode materials in constructed wetland incorporating microbial fuel cell. Bioresour Technol 2016;221:697–702.
[11] Saheb-Alam S, Persson F, Wilén B-M, Hermansson M, Modin O. Response to starvation and microbial community composition in microbial fuel cells enriched on different electron donors. Microb Biotechnol 2019;12(5):962–75.
[12] Zhou J, Liu W, Deng Y, Jiang Y-H, Xue K, He Z, Nostrand JDV, Wu L, Yang Y, Wang A, Handelsman J. Stochastic assembly leads to alternative communities with distinct functions in a bioreactor microbial community. mBio 2013;4(2):e00584-00512.
[13] Evans S, Martiny JBH, Allison SD. Effects of dispersal and selection on stochastic assembly in microbial communities. ISME J 2017;11(1):176–85.
[14] Krishnamurthy A, Gadhamshetty V, Mukherjee R, Chen Z, Ren W, Cheng HM, Koratkar N. Passivation of microbial corrosion using a graphene coating. Carbon 2013;56:45–9.
[15] Yu F, Wang C, Ma J. Applications of graphene-modified electrodes in microbial fuel cells. Materials 2016;9(10).
[16] He YR, Xiao X, Li WW, Sheng GP, Yan FF, Yu HQ, Yuan H, Wu LJ. Enhanced electricity production from microbial fuel cells with plasma-modified carbon paper anode. Phys Chem Chem Phys 2012;14(28):9966–71.
[17] Baranitharan E, Khan MR, Prasad DMR, Salihon JB. Bioelectricity generation from palm oil mill effluent in microbial fuel cell using polacrylonitrile carbon felt as electrode. Water, Air, Soil Pollut 2013;224(5):1533.
[18] Geim AK, Novoselov KS. The rise of graphene. Nat Mater 2007;6(3):183–91.
[19] McAllister MJ, Li J-L, Adamson DH, Schniepp HC, Abdala AA, Liu J, Herrera-Alonso M, Milius DL, Car R, Prud'homme RK, Aksay IA. Single sheet functionalized graphene by oxidation and thermal expansion of graphite. Chem Mater 2007;19(18):4396–404.
[20] Pumera M. Electrochemistry of graphene: new horizons for sensing and energy storage. Chem Rec 2009;9(4):211–23.
[21] Liu J, Qiao Y, Guo CX, Lim S, Song H, Li CM. Graphene/carbon cloth anode for high-performance mediatorless microbial fuel cells. Bioresour Technol 2012;114:275–80.
[22] Wang Y, Zhao CE, Sun D, Zhang JR, Zhu JJ. A graphene/poly(3,4-ethylenedioxythiophene) hybrid as an anode for high-performance microbial fuel cells. Chempluschem 2013;78(8):823–9.
[23] Dai H, Yang H, Liu X, Jian X, Liang Z. Electrochemical evaluation of nano-Mg(OH)2/graphene as a catalyst for hydrogen evolution in microbial electrolysis cell. Fuel 2016;174:251–6.
[24] Perreault F, Tousley ME, Elimelech M. Thin-film composite polyamide membranes functionalized with biocidal graphene oxide nanosheets. Environ Sci Technol Lett 2014;1(1):71–6.
[25] Wang L, Yuan Z, Karahan HE, Wang Y, Sui X, Liu F, Chen Y. Nanocarbon materials in water disinfection: state-of-the-art and future directions. Nanoscale 2019;11(20):9819–39.
[26] Firouzjaei MD, Seyedpour SF, Aktij SA, Giagnorio M, Bazrafshan N, Mollahosseini A, Samadi F, Ahmadalipour S, Firouzjaei FD, Esfahani MR, Tiraferri A, Elliott M, Sangermano M, Abdelrasoul A, McCutcheon JR, Sadrzadeh M, Esfahani AR, Rahimpour A. Recent advances in functionalized polymer membranes for biofouling control and mitigation in forward osmosis. J Membr Sci 2020;596:117604.
[27] Kumar S, Chatterjee K. Comprehensive review on the use of graphene-based substrates for regenerative medicine and biomedical devices. ACS Appl Mater Interfaces 2016;8(40):26431–57.
[28] Xia MY, Xie Y, Yu CH, Chen GY, Li YH, Zhang T, Peng Q. Graphene-based nanomaterials: the promising active agents for antibiotics-independent antibacterial applications. J Contr Release 2019;307:16–31.
[29] Saheb-Alam S, Singh A, Hermansson M, Persson F, Schnürer A, Wilén B-M, Modin O, Drake HL. Effect of start-up strategies and electrode materials on carbon dioxide reduction on biocathodes. Appl Environ Microbiol 2018;84(4):e02242-02217.
[30] Marshall CW, Ross DE, Fichot EB, Norman RS, May HD. Electrosynthesis of commodity chemicals by an autotrophic microbial community. Appl Environ Microbiol 2012;78(23):8412–20.
[31] Chen S, Zhou Y, Chen Y, Gu J. fastp: an ultra-fast all-in-one FASTQ preprocessor. Bioinformatics 2018;34(17):i884–90.
[32] Li D, Liu CM, Luo R, Sadakane K, Lam TW. MEGAHIT: an ultra-fast single-node solution for large and complex metagenomics assembly via succinct de Bruijn graph. Bioinformatics 2015;31(10):1674–6.
[33] Langmead B, Salzberg SL. Fast gapped-read alignment with Bowtie 2. Nat Methods 2012;9(4):357–9.
[34] Kang DD, Li F, Kirton E, Thomas A, Egan R, An H, Wang Z. MetaBAT 2: an adaptive binning algorithm for robust and efficient genome reconstruction from metagenome assemblies. PeerJ 2019;7:e7359.
[35] Li H. Minimap2: pairwise alignment for nucleotide sequences. Bioinformatics 2018;34(18):3094–100.
[36] Nissen JN, Johansen J, Allesøe RL, Sønderby CK, Armenteros JJA, Grønbech CH, Jensen LJ, Nielsen HB, Petersen TN, Winther O, Rasmussen S. Improved metagenome binning and assembly using deep variational autoencoders. Nat Biotechnol 2021.
[37] Parks DH, Imelfort M, Skennerton CT, Hugenholtz P, Tyson GW. CheckM: assessing the quality of microbial genomes recovered from isolates, single cells, and metagenomes. Genome Res 2015;25(7):1043–55.
[38] Chaumeil P-A, Mussig AJ, Hugenholtz P, Parks DH. GTDB-Tk v2: memory friendly classification with the genome taxonomy database. Bioinformatics 2022;38(23):5315–6.
[39] Jain C, Rodriguez-R LM, Phillippy AM, Konstantinidis KT, Aluru S. High throughput ANI analysis of 90K prokaryotic genomes reveals clear species boundaries. Nat Commun 2018;9(1):5114.
[40] Chao A, Chiu C-H, Jost L. Unifying species diversity, phylogenetic diversity, functional diversity, and related similarity and differentiation measures through Hill numbers. Annu Rev Ecol Evol Syst 2014;45(1):297–324.
[41] Modin O, Liébana R, Saheb-Alam S, Wilén B-M, Suarez C, Hermansson M, Persson F. Hill-based dissimilarity indices and null models for analysis of microbial community assembly. Microbiome 2020;8(1):132.
[42] Pielou EC. The measurement of diversity in different types of biological collections. J Theor Biol 1966;13:131–44.
[43] Seabold S, Perktold J. statsmodels: econometric and statistical modeling with python. In: 9th Python in science conference; 2010.
[44] Virtanen P, Gommers R, Oliphant TE, Haberland M, Reddy T, Cournapeau D, Burovski E, Peterson P, Weckesser W, Bright J, van der Walt SJ, Brett M, Wilson J, Millman KJ, Mayorov N, Nelson ARJ, Jones E, Kern R, Larson E, Carey CJ, Polat I, Feng Y, Moore EW, VanderPlas J, Laxalde D, Perktold J, Cimrman R, Henriksen I, Quintero EA, Harris CR, Archibald AM, Ribeiro AH, Pedregosa F, van Mulbregt P, SciPy 1.0 Contributors. SciPy 1.0: fundamental algorithms for scientific computing in Python. Nat Methods 2020;17:261–72.
[45] Azen R, Budescu DV. The dominance analysis approach for comparing predictors in multiple regression. Psychol Methods 2003;8(2):129–48.
[46] McKinney W, others. Data structures for statistical computing in python. Proc 9th Python Sci Conf 2010;445:51–6.
[47] R Core Team. R: a language and environment for statistical computing. Vienna, Austria: R Foundation for Statistical Computing; 2020.
[48] Oksanen J SG, Blanchet F, Kindt R, Legendre P, Minchin P, O'Hara R, Solymos P, Stevens M, Szoecs E, Wagner H, Barbour M, Bedward M, Bolker B, Borcard D, Carvalho G, Chirico M, De Caceres M, Durand S, Evangelista H, FitzJohn R, Friendly M, Furneaux B, Hannigan G, Hill M, Lahti L, McGlinn D, Ouellette M, Ribeiro Cunha E, Smith T, Stier A, Ter Braak C, Weedon J. vegan: Community Ecology Package. R package version 2.6-4." from, https://CRAN.R-project.org/package=vegan; 2022.
[49] Yang G, Li Y, Lin A, Zhuang L. Geobacter benzoatilyticus sp. nov., a novel benzoate-oxidizing, iron-reducing bacterium isolated from petroleum contaminated soil. Int J Syst Evol Microbiol 2022;72(3).
[50] Jost L. Entropy and diversity. Oikos 2006;113(2):363–75.
[51] De-la-Pinta I, Cobos M, Ibarretxe J, Montoya E, Eraso E, Guraya T, Quindós G. Effect of biomaterials hydrophobicity and roughness on biofilm development. J Mater Sci Mater Med 2019;30(7):77.
[52] Pandit S, Cao Z, Mokkapati VRSS, Celauro E, Yurgens A, Lovmar M, Westerlund F, Sun J, Mijakovic I. Vertically aligned graphene coating is bactericidal and prevents the formation of bacterial biofilms. Adv Mater Interfac 2018;5(7):1701331.
[53] Pandit S, Gaska K, Kádár R, Mijakovic I. Graphene-based antimicrobial biomedical surfaces. ChemPhysChem 2021;22(3):250–63.
[54] Abadikhah M, Rodriguez MdC, Persson F, Wilén B-M, Farewell A, Modin O. Evidence of competition between electrogens shaping electroactive microbial communities in microbial electrolysis cells. Front Microbiol 2022;13.
[55] Niederdorfer R, Fragner L, Yuan L, Hausherr D, Wei J, Magyar P, Joss A, Lehmann MF, Ju F, Bürgmann H. Distinct growth stages controlled by the interplay of deterministic and stochastic processes in functional anammox biofilms. Water Res 2021;200:117225.
[56] Lee H-S, Torres CI, Rittmann BE. Effects of substrate diffusion and anode potential on kinetic parameters for anode-respiring bacteria. Environ Sci Technol 2009;43(19):7571–7.
[57] Reguera G, McCarthy KD, Mehta T, Nicoll JS, Tuominen MT, Lovley DR. Extracellular electron transfer via microbial nanowires. Nature 2005;435(7045):1098–101.
[58] Reguera G, Nevin KP, Nicoll JS, Covalla SF, Woodard TL, Lovley DR. Biofilm and nanowire production leads to increased current in Geobacter sulfurreducens fuel cells. Appl Environ Microbiol 2006;72(11):7345–8.
[59] Cai W, Liu W, Han J, Wang A. Enhanced hydrogen production in microbial electrolysis cell with 3D self-assembly nickel foam-graphene cathode. Biosens Bioelectron 2016;80:118–22.
[60] Liu S, Zeng TH, Hofmann M, Burcombe E, Wei J, Jiang R, Kong J, Chen Y. Antibacterial activity of graphite, graphite oxide, graphene oxide, and reduced graphene oxide: membrane and oxidative stress. ACS Nano 2011;5(9):6971–80.
[61] Ruiz ON, Fernando KA, Wang B, Brown NA, Luo PG, McNamara ND, Vangsness M, Sun YP, Bunker CE. Graphene oxide: a nonspecific enhancer of cellular growth. ACS Nano 2011;5(10):8100–7.
[62] Liao C, Li Y, Tjong SC. Graphene nanomaterials: synthesis, biocompatibility, and cytotoxicity. Int J Mol Sci 2018;19(11).
[63] Sasaki K, Morita M, Hirano S, Ohmura N, Igarashi Y. Effect of adding carbon fiber textiles to methanogenic bioreactors used to treat an artificial garbage slurry. J Biosci Bioeng 2009;108(2):130–5.

[64] Tsai H-Y, Wu C-C, Lee C-Y, Shih EP. Microbial fuel cell performance of multiwall carbon nanotubes on carbon cloth as electrodes. J Power Sources 2009;194(1):199–205.
[65] Zahran RR. Electrical conductivity of nickel reinforced graphite electrodes. Mater Lett 1991;10(9):461–4.
[66] Chao A, Chiu C-H, Jost L. Phylogenetic diversity measures based on Hill numbers. Phil Trans Roy Soc Lond B Biol Sci 2010;365(1558):3599–609.
[67] Bond DR, Lovley DR. Electricity production by *Geobacter sulfurreducens* attached to electrodes. Appl Environ Microbiol 2003;69(3):1548–55.
[68] Wang N, Yang Y, Xu K, Long X, Zhang Y, Liu H, Chen T, Li J. Distinguishing anaerobic digestion from electrochemical anaerobic digestion: metabolic pathways and the role of the microbial community. Chemosphere 2023;326:138492.
[69] Katuri KP, Kamireddy S, Kavanagh P, Muhammad A, Conghaile PÓ, Kumar A, Saikaly PE, Leech D. Electroactive biofilms on surface functionalized anodes: the anode respiring behavior of a novel electroactive bacterium, Desulfuromonas acetexigens. Water Res 2020;185:116284.
[70] Janssen PH, Ofarrell KA. Succinispira mobilis gen. nov., sp. nov., a succinate-decarboxylating anaerobic bacterium. Int J Syst Evol Microbiol 1999;49(3):1009–13.